Available online at www.sciencedirect.com
SCIENCE DIRECT®
Advances in Space Research 36 (2005) 906–914
ADVANCES IN SPACE RESEARCH (a COSPAR publication)
www.elsevier.com/locate/asr

Lunar occultation with SCIAMACHY: First retrieval results

L.K. Amekudzi *, A. Bracher, J. Meyer, A. Rozanov, H. Bovensmann, J.P. Burrows

Department of Physics and Electrical Engineering, Institute of Environmental Physics/Remote Sensing, University of Bremen, P.O. Box 330440, Otto-Hahn-Allee 1, D-28359 Bremen, Germany

Received 6 September 2004; received in revised form 8 February 2005; accepted 3 March 2005

Abstract

Scanning imaging absorption spectrometer for atmospheric chartography (SCIAMACHY) is a moderate resolution imaging spectrometer on board the environmental satellite (ENVISAT) launched in March 2002. SCIAMACHY has eight channels, covering a spectral range from 240 to 2380 nm and observes the Earth's atmosphere in nadir, limb, and occultation geometries. From SCIAMACHY lunar occultation measurements, nighttime vertical profiles of O_3 and NO_2 have been retrieved over the southern hemisphere (60°–90°S) using the optimal estimation method. The first preliminary validation of retrieved O_3 profiles with halogen occultation experiment and comparisons with stratospheric aerosol and gas experiment III (SAGE III), and Michelson interferometer for passive atmospheric sounding (MIPAS) O_3 profiles were carried out. In addition, the retrieved NO_2 profiles were compared to SAGE III and MIPAS results. The results of these preliminary validation and comparisons give confidence that reasonable scientific data products (trace gas profiles) can be derived from SCIAMACHY spectroscopic lunar occultation data.

Keywords: Lunar occultation measurement; O_3 and NO_2 vertical profile; SCIAMACHY; ENVISAT; Atmospheric physics and chemistry

1. Introduction

The discovery of the ozone hole (Farman et al., 1985) and the depletion of ozone layer by chemically active species in the stratosphere necessitate a global long-term monitoring of ozone. NO_2 and O_3 are key molecules involved in the ozone chemistry in the stratosphere. NO_2 reacts with O_3 to produce a radical, NO_3. This is removed from the atmosphere by reacting with NO_2 to form N_2O_5 (a temperature dependent equilibrium reaction). In polar winters, N_2O_5 reacts on the surface of stratospheric sulphate aerosol (SSA) heterogeneously to form HNO_3 which is a long lived reservoir for NO_x ($NO + NO_2$) in the stratosphere (Wayne et al., 1991). To fully understand the contribution of NO_x to long-term ozone loss process in the stratosphere, it is important to measure simultaneously the concentrations of NO_2 and O_3 in the stratosphere. The lunar occultation measurement technique is an excellent method to contribute to this objective.

Nighttime measurements of trace gases (O_3 and NO_2) using lunar occultation method have been performed successfully by ground based sensors and balloon platforms and the results have been reported by several authors, see for example (Solomon et al., 1994; Poisson et al., 2001). These measurements however, have not provided broader geographical coverage of the atmospheric trace species. Recent satellite platforms have introduced lunar occultation methods to measure nighttime atmospheric trace gases; these instruments are scanning imaging absorption spectrometer for atmospheric chartography (SCIAMACHY) and stratospheric aerosol and gas experiment III (SAGE III).

SCIAMACHY is a moderate resolution spectrometer on board the environmental satellite (ENVISAT)

* Corresponding author. Tel.: +49 421 2183223; fax: +49 421 2184555.
E-mail address: leonard@iup.physik.uni-bremen.de (L.K. Amekudzi).

0273-1177/$30
doi:10.1016/j.asr.2005.03.017

launched in March 2002 from Kourou, French Guiana. The instrument was developed to contribute to better understanding of ozone chemistry, pollution and climate monitoring issues. SCIAMACHY has eight channels, covering a spectral range of 240–2380 nm, with a spectral resolution of 0.24–1.48 nm. The instrument measures scattered, reflected and transmitted radiation in nadir, limb, and occultation geometries (Bovensmann et al., 1999).

The goal of this paper is to present the first results of O_3 and NO_2 density profiles retrieved from SCIAMACHY lunar occultation uncalibrated (level-0) data and the preliminary validation performed for these species.

2. Lunar occultation measurements and data

2.1. Lunar occultation measurements

The SCIAMACHY instrument performs lunar occultation measurements in the southern hemisphere of the Earth's atmosphere, between 30° and 90° latitude, during local nighttime. SCIAMACHY moon visibility is possible above the northern hemisphere however, these events usually coincide with sunrise. Also the lunar phase is less than 0.5, therefore it is impossible to perform useful lunar measurements. While sunrise is mainly defined by the relatively stable position of the Sun with respect to ENVISAT's orbital plane, the properties of moonrise in SCIAMACHY's limb field of view (LFOV) are determined by the orientation of the lunar orbital plane with respect to ENVISAT's orbital plane and the ecliptic. In this plane, the moon completes one orbit within one synodic period of 29.53 days. Caused by the lunar orbital motion, the moon moves through the LFOV from left to right at a rate of about 1° per orbit, starting lunar occultation measurement at a lunar phase of 0.6–0.7 and ending shortly after full moon. These measurements are performed in moon pointing (staring) mode similar to halogen occultation experiment (HALOE) (Russel et al., 1993). The SCIAMACHY instrument's instantaneous field of view (IFOV) in lunar occultation mode is 0.045° in vertical direction (height) and 1.8° in horizontal direction, the later is larger than the apparent diameter of the moon, which is approximately 0.5°. To effectively track the moon, the moon follower (MF) device is adjusted to the brightest point of the apparent moon, as the moon rises above the Earth's horizon. Starting at ≈17 km, the MF follows the moon up to 100 km (Noël et al., 2000). Below this critical altitude of 17 km, apparent angular rate of the rising true moon is significantly higher than that of the rising refracted images, as a result, tracking the rising moon become almost impossible for the MF. Above 100 km moon measurements are performed for instrument calibration purposes. The integration time for SCIAMACHY lunar occultation measurement is 1.0 s and the vertical resolution is ≈3 km.

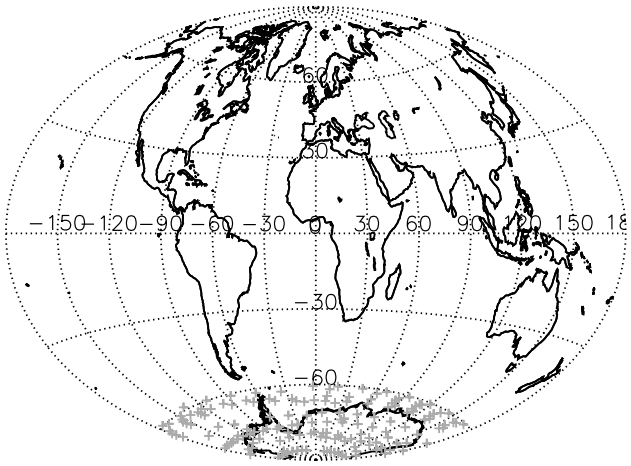

Fig. 1. SCIAMACHY lunar occultation geographical coverage for 2003. The grey crosses indicate the location of measurements.

SCIAMACHY lunar occultation can be successfully executed only when the lunar visibility occurs on the nightside. Due to the large field of view (2.1° × 2.1°), the MF always detects in dayside occultations, additionally to the moonlight, a strong signal from the bright Earth atmosphere at lower lunar altitudes. This prevents MF control from acquiring and tracking the moon. In addition, variability in the lunar albedo, the perturbation effect of the motion of the moon, and seasons are other challenges faced by interpretation of SCIAMACHY lunar occultation data (ESA, 1994). The useful SCIAMACHY lunar occultation events where the moon rises on the nightside are on the average 6 days per month and 3–6 months in the year. Lunar occultation measurements performed in 2003 are located in the latitude band of 60°–90 °S (see Fig. 1), These measurements were carried out from February to June 2003 (see Fig. 2).

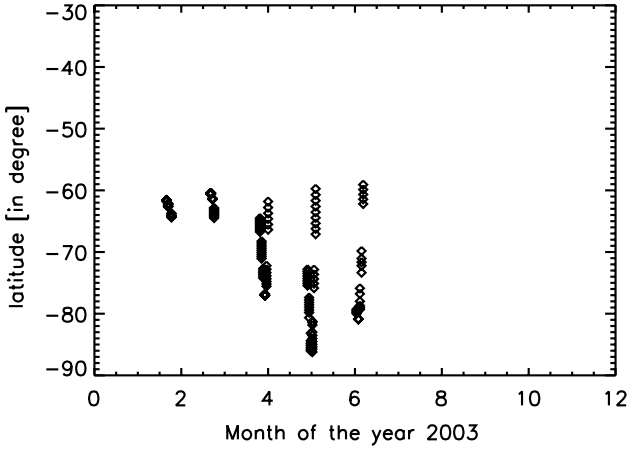

Fig. 2. Latitude for each measurement as a function of the month (February–June) of the year 2003.

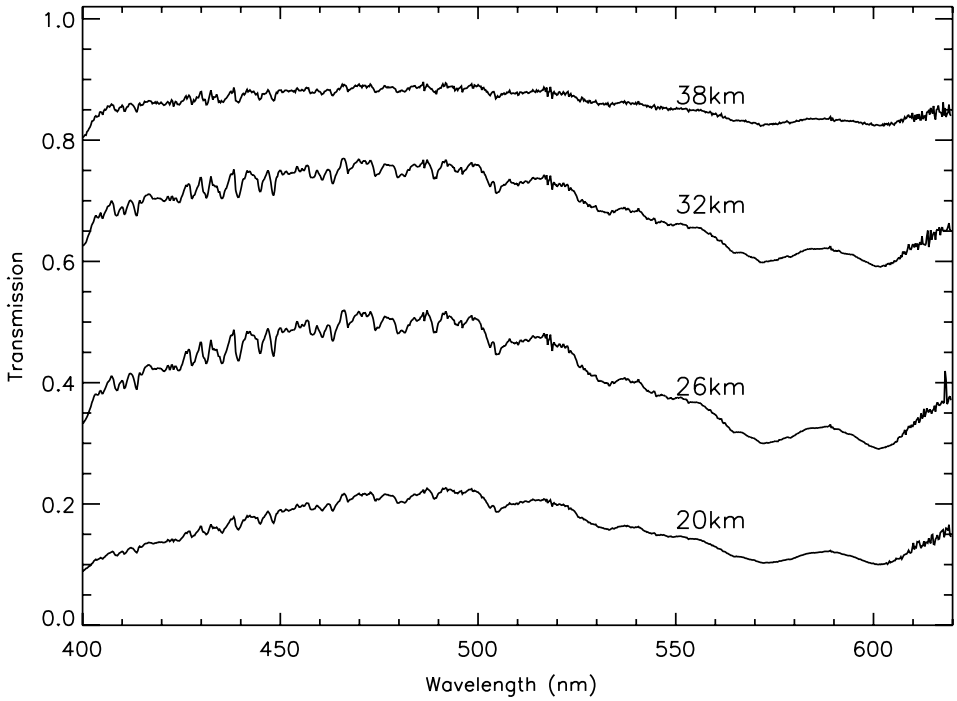

Fig. 3. The measured SCIAMACHY lunar transmission spectra for selected altitudes. These spectra correspond to measurements of orbit number 5390 and SZA = 105.8°, taken on 12th of March 2003.

2.2. Spectroscopic data source

The data used for the retrieval were extracted from the uncalibrated (level-0) SCIAMACHY lunar occultation data. The extraction involves removal of dead pixels, dark current correction, and wavelength calibration. This is followed by the extraction of lunar spectrum at each tangent height and spectral point, starting from 17 to 100 km and extraction of the lunar reference spectrum (measurements above 100 km). The transmission spectra, containing atmospheric spectral lines are obtained by dividing the measured lunar occultation spectrum at a given line of sight by the measured lunar reference spectrum. Fig. 3 shows an example of the measured lunar transmission spectra of the spectral region of interest (400–620 nm) for selected altitudes.

3. Retrieval methodology and results

In this section, data analysis technique, source of a priori data, and retrieval results are presented.

3.1. Data analysis

A detailed description of the retrieval scheme for occultation data analysis is given by (Rozanov, 2001). In this scheme, the forward model used to derive the simulated transmission and the Jacobian is based on Lambert–Beer's law. The simulated transmission $\Upsilon^{s}(h_i, \lambda)$ for a given tangent height, h_i, and wavelength, λ, is given by

$$\Upsilon^{s}(h_i, \lambda) = \int_{\Omega} \int_{\Delta\lambda} S(\lambda, \lambda') F(\omega) e^{-\tau(h_i, \lambda')} \, d\lambda' \, d\omega, \qquad (1)$$

where $\Delta\lambda$ is the total width of SCIAMACHY slit function $S(\lambda, \lambda')$, Ω is the field of view of the instrument and $F(\omega)$ is the apparatus function. $\tau(h_i, \lambda')$ is the full optical depth along the line of sight through the atmosphere.

O_3 and NO_2 were fitted together using the spectral window of 425–600 nm (channel three of SCIAMACHY instrument) containing the differential absorption structure of O_3 and NO_2. The visible window was used for the retrieval as the SCIAMACHY lunar data has higher signal-to-noise ratio in the visible region than in the ultraviolet region.

To remove broadband absorption features of the atmosphere and instrument from the measured spectra, a polynomial of third-order is subtracted. This is done for the logarithms of measured and reference lunar occultation radiances at each line of sight, the logarithm of simulated transmission spectra and the logarithmic weighting functions. Further, shift and squeeze correction is performed to reduce uncertainties associated with wavelength calibration and doppler shift. Furthermore the quadratic form of the resulting differential transmission spectra was minimised.

Fig. 4 shows the spectral fits of NO_2 and O_3 at 27 km tangent height for April 12, 2003, corresponding to

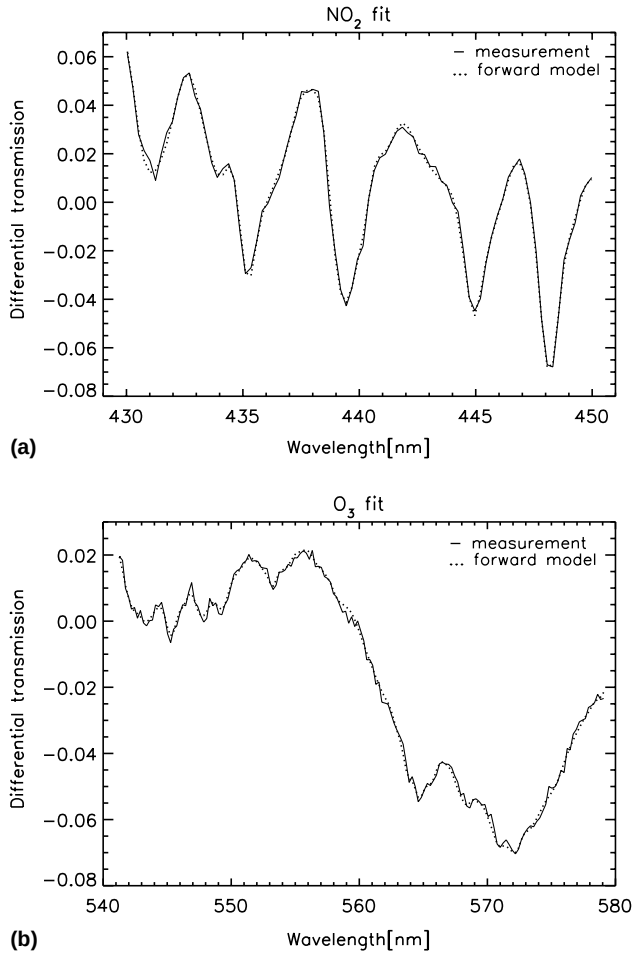

Fig. 4. The spectral fit at 27 km tangent height (for April 12, 2003, orbit number = 5828, and SZA = 115°). The dotted line represents the modeled differential transmission spectrum and the solid line is the measured differential transmission spectrum: (a) NO_2 fits; (b) O_3 fits.

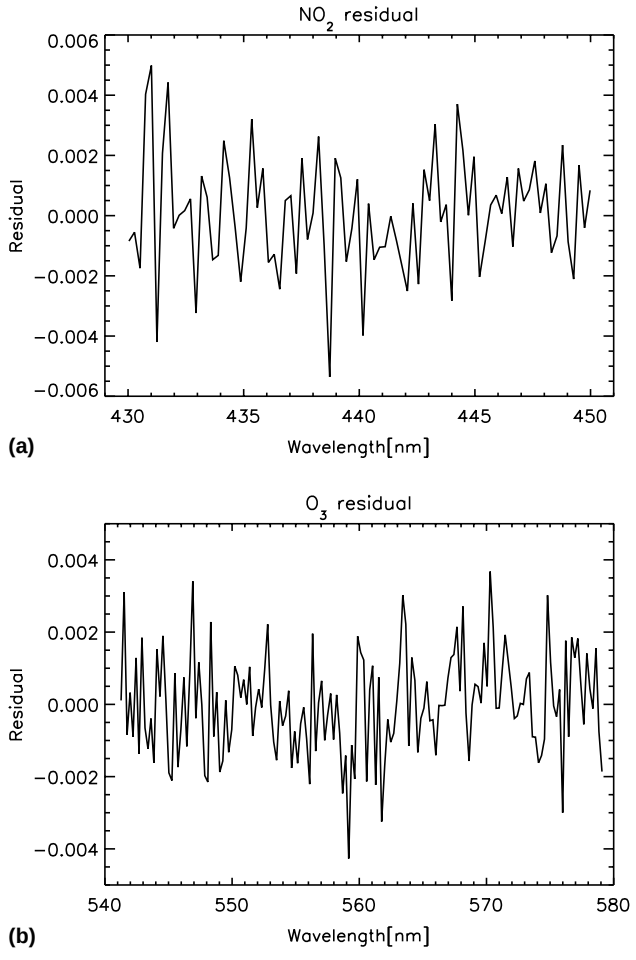

Fig. 5. (a) NO_2 residual at 27 km tangent height. The residual of NO_2 is in the order of 0.4% for all relevant height layers. (b) O_3 residual at 27 km tangent height. The residual of O_3 is in the order of 0.2% for all relevant height layers.

ENVISAT orbit number 5828 and solar zenith angle (SZA) of 115°. Fig. 4(a) presents an example of the spectral fit of NO_2 covering the spectral band of 430–450 nm and Fig. 4(b) is the spectral fit of O_3 covering the spectral band of 540–580 nm. The dotted lines are the simulated differential transmission spectra and the solid lines are the measured differential transmission spectra. The spectral fits are of high quality and show absorption features mainly due to NO_2 and O_3.

The residual of the retrieval, i.e., the difference between the measured and the simulated differential transmission spectra is shown in Fig. 5. Fig. 5(a) shows the corresponding spectral residual of NO_2 spectral fit and Fig. 5(b) shows the corresponding spectral residual of O_3 spectral fit. In an ideal case, where the transmission is perfectly modeled, the residual should reflect the signal-to-noise ratio of the measurement. The quality of the retrieval therefore can be inferred from the residual. The residual of O_3 and NO_2 spectral fit are in the order of 0.2% and 0.4%, respectively, for all relevant height layers. These values are reasonable and agree favorably with the signal-to-noise ratio of the measurements.

Finally, number density profiles of the fitted trace gases are derived by inverting the linear path integral in Eq. (1) iteratively following the Newton iteration scheme, using the optimal estimation method (OEM) (Rodgers, 1976).

3.2. A priori data source

The geometric height is used as vertical coordinate for both the forward model and the inversion scheme. The atmosphere is divided into 100 equidistant layers between 0 and 100 km altitude. O_3 and NO_2 absorption cross-sections at five different temperatures measured at University of Bremen (Burrows et al., 1998) were used. Temperature, pressure, NO_2 and O_3 a priori profiles were taken from the US standard atmosphere (NASA, 1976).

In occultation geometry, the line of sight geometry is uniquely defined by its tangent height. The tangent

height information is provided along side the spectroscopic data by European Space Agency (ESA), however this information sometimes have tangent height shift of about 1 km due to misalignments of pre-calculated detector pointing geometry and refractive effects at lower tangent heights. The tangent height information are improved by an independent fitting and subsequent retrieval of O_2 profiles (Meyer et al., 2005) using O_2-A-bands spectral window.

3.3. Averaging kernel and precision

The averaging kernel matrix, A, is a quantity often used to describe the dependence of the retrieved atmospheric state vector, $\hat{x}$, on variations of the true atmospheric state vector, x, A is given as

$$A = \frac{\partial \hat{x}}{\partial x}. \tag{2}$$

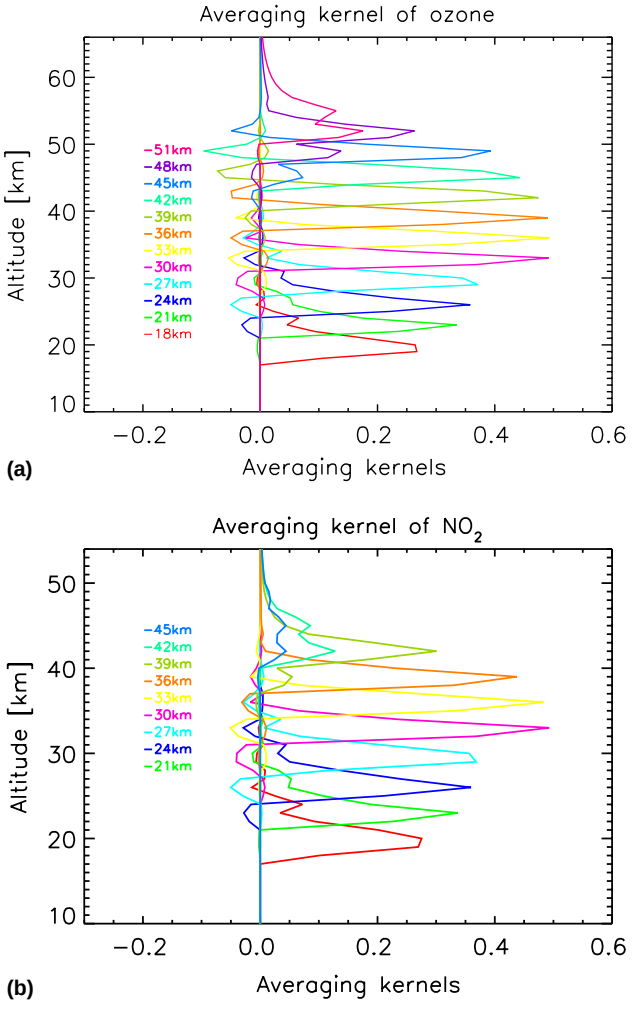

Fig. 6. Averaging kernnels of selected altitudes for O_3 and NO_2 retrieved profiles (1 km retrieval grid): (a) O_3 averaging kernel; (b) NO_2 averaging kernel.

Usually, the vertical resolution of each retrieval is characterised by examining the averaging kernel element that couple the true profile and the retrieved profile of a given trace gas. In the OEM scheme, the complete retrieval process is assumed to be linear with respect to the atmospheric state vector given as

$$\hat{x} = Ax + (I - A)x_0 + \varepsilon, \tag{3}$$

where I is the unit matrix, x_0 is the a priori state vector, and ε is all possible errors (Rodgers, 1990). For an ideal scenario, A is a unit matrix, but in reality the rows of A are peaked functions with finite width. The width is regarded as a measure of the vertical resolution of the retrieved profiles. As an example, averaging kernels for selected altitudes for retrieved O_3 and NO_2 are shown in Fig. 6. The averaging kernels show that O_3 information can be retrieved from SCIAMACHY lunar occultation measurement in the altitude range of 18–50 km and NO_2 can be retrieved in the altitude range of 18–40 km.

Precision of the retrieved O_3 and NO_2 profiles were calculated using a priori covariance of 95% and signal to noise ratio of 2000. In the absence of systematic error, O_3 vertical profile distribution can be retrieved from

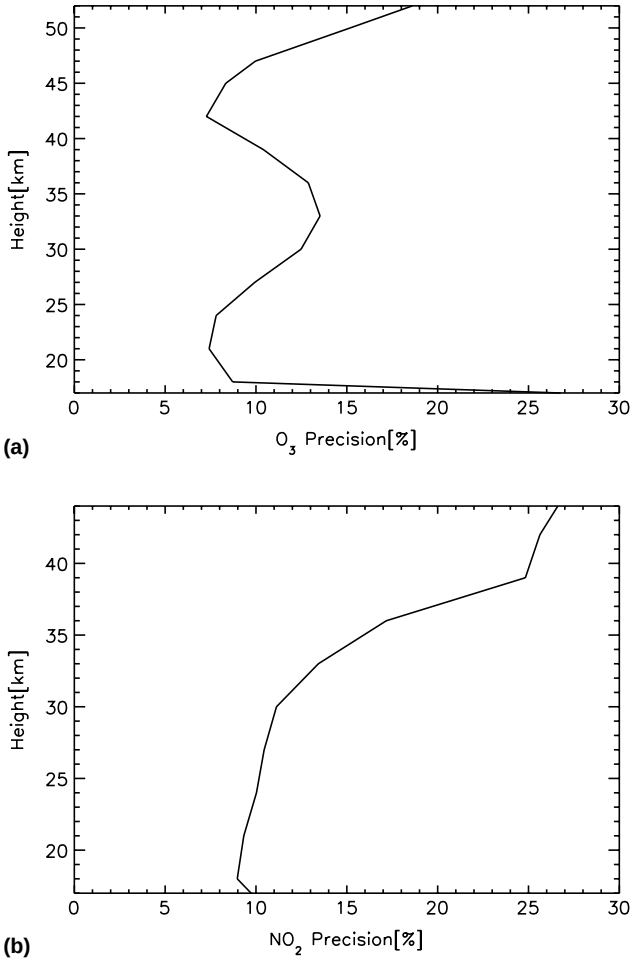

Fig. 7. Precision of retrieved O_3 and NO_2 number density profiles (3 km measurement grid), O_3 precision (a) and NO_2 precision (b).

SCIAMACHY lunar occultation data with an accuracy better than 13% between 18 and 50 km and NO_2 vertical profiles with an accuracy better than 20% between 18 and 40 km (see Fig. 7).

3.4. SCIAMACHY–SAGE III O_3 and NO_2 comparison

O_3 and NO_2 number density profiles derived from SCIAMACHY lunar occultation spectroscopic data are compared with collocated SAGE III lunar occultation retrieved profiles. Coincident measurements were taken on the same day, using data sets with latitudinal and longitudinal difference of 5° and 10°, respectively. These measurements were taken on the 12th of April, 2003. Fig. 8 shows the comparison of the mean number density profiles of 9 collocated SCIAMACHY and SAGE III O_3 and NO_2 profiles. O_3 results are in good agreement with SAGE III results, SCIAMACHY result is slightly lower (2–8%) than SAGE III result. NO_2 results, however, show higher concentrations for SCIAMACHY between 20 and 40 km. Due to strong diurnal variation of NO_2, difference in local time (LT) or SZA of measurement could lead to a some difference in the NO_2 concentration. SAGE III measurement were taken between 18 and 19 h LT corresponding to SZA between 96° and 100°, whereas SCIAMACHY measurements were taken between 21 and 22 h LT corresponding to SZA between 114° and 115°. NO_2 results are however promising because just after sunset concentration of NO_2 is expected to be lower than the concentration later in the night (Brasseur et al., 1999).

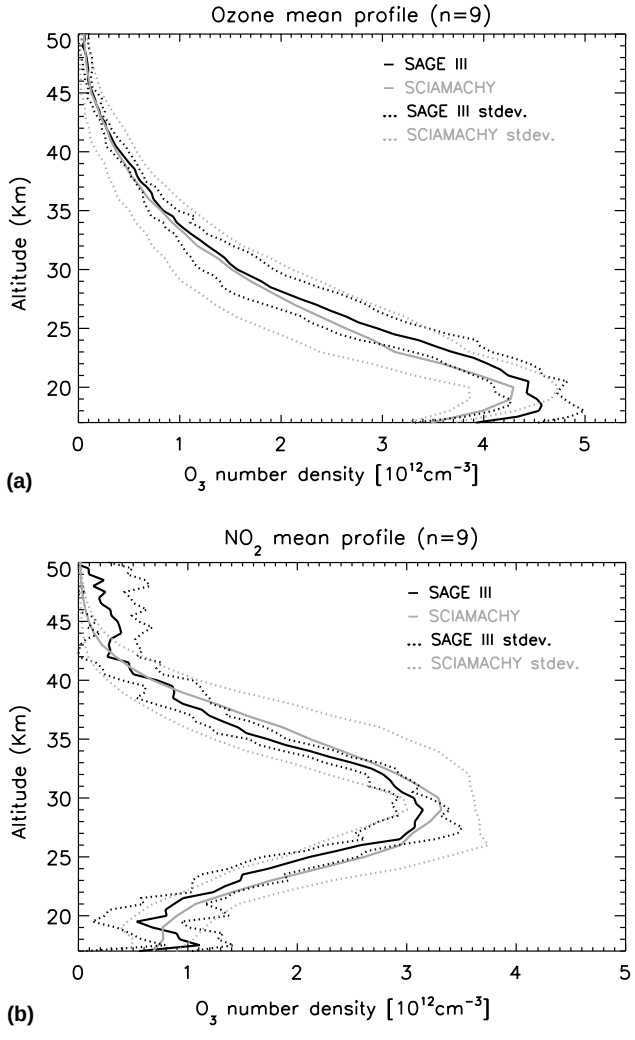

Fig. 8. (a) The mean O_3 density profile of 9 collocated events and (b) the mean NO_2 density profile of 9 collocated events. SCIAMACHY (grey solid line) and SAGE III (black solid line) and the dotted lines are the standard deviations with respect to the mean.

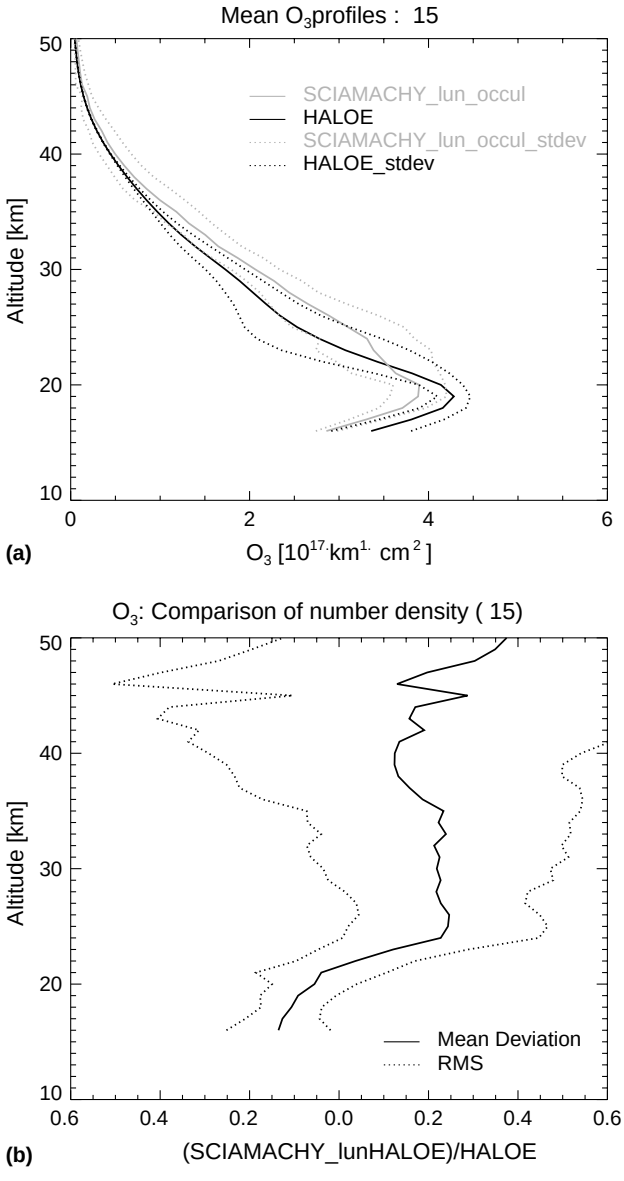

Fig. 9. The mean O_3 density profile for 15 collocated events is shown (a), grey SCIAMACHY and black HALOE. The mean relative deviation (solid line) and the RMS of the mean relative deviation (dotted line) of the comparison of 15 collocated SCIAMACHY O_3 profiles with HALOE is shown (b).

3.5. SCIAMACHY–HALOE O_3 validation

Results of SCIAMACHY retrieved O_3 profiles are compared with HALOE retrieved O_3 profiles as a preliminary validation. This validation was based on 15 single collocated measurements. Due to poor geographical coincidence, large distances between matched measurements were considered. These distances were between 600 and 1000 km. The collocated events were taken on 13th and 14th of March, 2003.

Fig. 9 shows the statistical results of the comparison of SCIAMACHY O_3 profiles with HALOE. There is a positive bias of SCIAMACHY to HALOE mean O_3 density profiles in the middle stratosphere (25–45 km). The mean relative deviations is in the range of +10–20% of SCIAMACHY to HALOE and RMS is in the range of 10–30% for altitude range of 17–45 km.

3.6. SCIAMACHY–MIPAS O_3 and NO_2 comparison

Figs. 10 and 11 show statistical results of collocated SCIAMACHY and Michelson interferometer for passive atmospheric sounding (MIPAS) O_3 and NO_2 number density profiles. The distances between collocated events were in the range of 40–600 km and these measurements were taken in March and April 2003. In addition, only SZA differences in the range of 1–4° between collocated events were considered for the NO_2

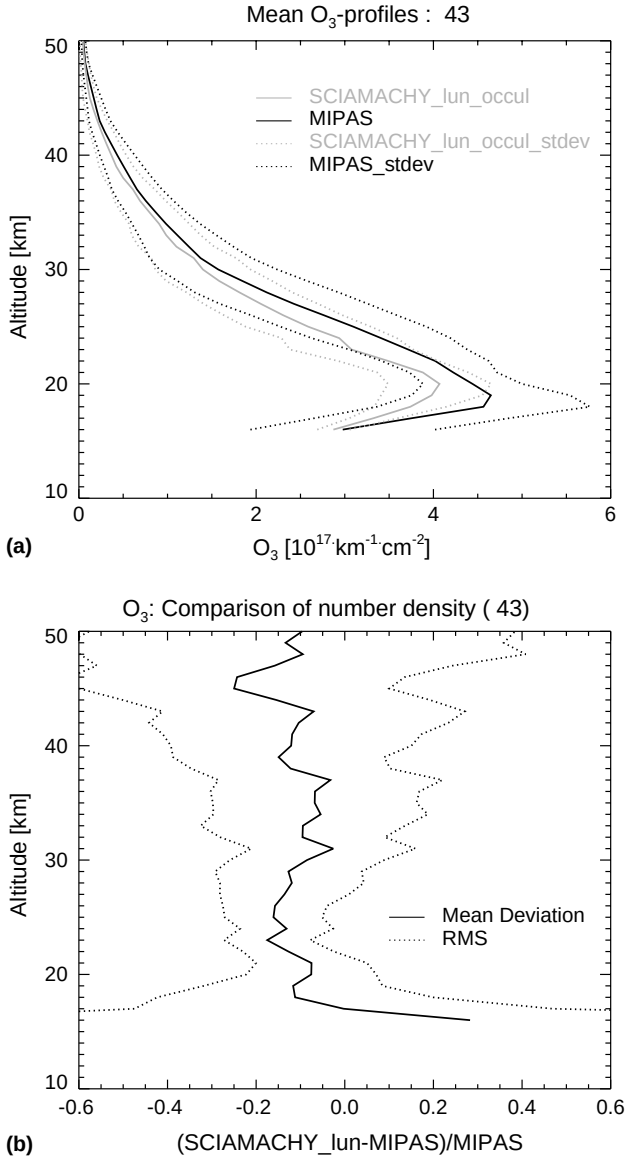

Fig. 10. The mean O_3 density profile for 43 collocated events is shown (a), grey SCIAMACHY and black MIPAS. The mean relative deviation (solid line) and the RMS of the mean relative deviation (dotted line) of the comparison of 43 collocated SCIAMACHY O_3 profiles with MIPAS is shown (b).

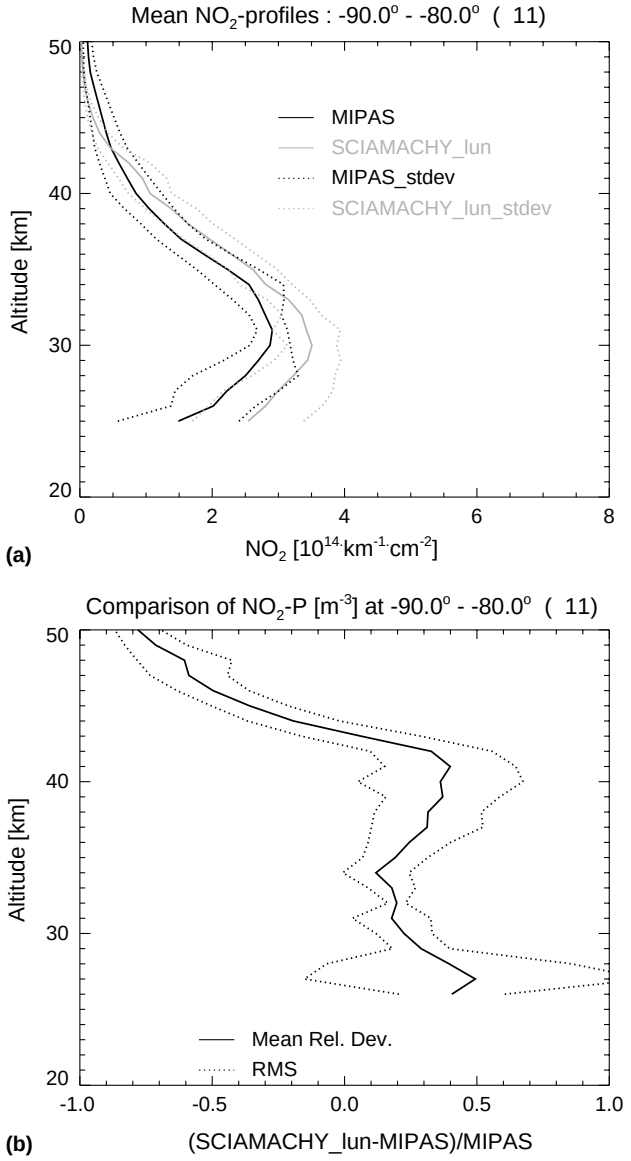

Fig. 11. The mean NO_2 density profile for 11 collocated events is shown (a), grey SCIAMACHY and black MIPAS. The mean relative deviation (solid line) and the RMS of the mean relative deviation (dotted line) of the comparison of 11 collocated SCIAMACHY NO_2 profiles with MIPAS is shown (b).

comparison. O_3 statistics is based on 43 single profiles and NO_2 statistics on 11 single profiles.

There is a slight negative bias of SCIAMACHY mean O_3 profiles compared to MIPAS between 18 and 45 km. The mean relative deviations of SCIAMACHY to MIPAS and the RMS of O_3 results are, respectively, in the range of −5 to −15% and 10–30% between 25 and 40 km. There is a positive bias of SCIAMACHY mean NO_2 profiles compared to MIPAS in the middle stratosphere (25–40 km). The mean relative deviations are in the range of +15–40% of SCIAMACHY to MIPAS and the RMS is in the range of 10–30% between 25 and 40 km.

4. Conclusion

In this paper, we have presented the first retrieved scientific data products of SCIAMACHY lunar occultation measurements. O_3 and NO_2 number density profiles have been retrieved using the OEM.

The spectral fits are of high quality and show absorption features of the fitted trace gases. The spectral residual are in the order of 0.2% and 0.4% for O_3 and NO_2, respectively. The averaging kernels show reasonable retrieval sensitivity for O_3 and NO_2. O_3 vertical profile distribution can be retrieved from 18 to 50 km with an accuracy better than 13%. Whereas NO_2 vertical profile distribution can be retrieved from 18 to 40 km with an accuracy better than 20%.

Comparisons of collocated SCIAMACHY O_3 profiles with HALOE show that the quality of O_3 retrieved from SCIAMACHY lunar occultation is high (within 10–20% between 25 and 48 km). There is good agreement of SCIAMACHY O_3 mean profile to MIPAS and SAGE III between 25 and 45 km. The mean deviations and RMS deviations of SCIAMACHY–MIPAS comparison are in the order of 10–15%, respectively. Concentration of NO_2 measured by SCIAMACHY instrument is slightly higher than that measured by SAGE III and MIPAS instruments, this may be due to difference in SZA or air masses analysed. The quality of our retrieved profiles is good, however, NO_2 profiles require further validation using photochemical corrections (Bracher et al., 2004), these comparisons would be carried out using POAM III NO_2 data. A complete validation of these results will improve our understanding of nighttime O_3 chemistry.

Acknowledgements

We are thankful to the following persons and Institutions: European Space Agency (ESA) for providing SCIAMACHY level-0 and MIPAS level-2 data. Stephan Noël for downloading SCIAMACHY level-0 data. HALOE group at Hampton University (especially J.M. Russell III) and NASA LaRC (especially E. Thompson). Ghassan Taha, University of Arizona and NASA Langley Research Center, USA for providing SAGE III scientific products. This work has been funded in parts by the German Ministry of Education and Research (BMBF) via grants 07ATF52, 07UFE12/8, FKZ01SF9994 and 50EE0025, the University of Bremen and the state of Bremen.

References

Bovensmann, H., Burrows, J.P., Buchwitz, M., Frerick, J., Noël, S., Rozanov, V.V., Chance, K.V., Goede, A.P.H. SCIAMACHY: mission objectives and measurement modes. J. Atmos. Sci. 56 (2), 127–150, 1999.

Bracher, A., Sinnhuber, M., Rozanov, A., Burrows, J.P. NO_2 Modelling used for the comparison of NO_2, satellite measurements at different solar zenith angles. Atmos. Chem. Phys. Discuss. 4, 5515–5548, 2004.

Brasseur, G.P., Orlando, J.J., Tyndall, G.S. (Eds.). Atmospheric Chemistry and Global Change. Oxford University Press, Oxford, 1999.

Burrows, J.P., Dehn, A., Deters, B., Himmelmann, S., Richter, A., Voigt, S., Orphal, J. Atmospheric remote-sensing reference data from GOME: 1. Temperature-dependent absorption cross sections of NO_2 in the 231–794 nm range. J. Quant. Spectrosc. Radiat. Trans. 60, 1025–1031, 1998.

ESA. Study of the Sun and Moon as radiation calibration targets. Tech. rep., Space Systems Finland Ltd., SF-02151 Espoo, Finland, 1994.

Farman, J.C., Gardner, B.G., Franklin, J.D. Large losses of total ozone in Antarctica reveal seasonal ClO_x and NO_x interaction. Nature 315, 207–210, 1985.

Meyer, J., Bracher, A., Rozanov, A., Schlesier, A.C., Bovensmann, H., Burrows, J.P. Solar occultation with SCIAMACHY: algorithm description and first validation. Atmos. Chem. Phys. Discuss. 5, 17–66, 2005.

NASA. U.S. standard atmosphere supplements. Tech. rep., U.S. Government Printing, Washington, DC, 1976.

Noël, S., Bovensmann, H., Wuttke, M.W., Burrows, J.P., Gottwald, M., Krieg, E., Mager, R. SCIAMACHY nominal operations and special features. Tech. rep., ERS-ENVISAT symposium, Gothenburg, 2000.

Poisson, N., et al. The impact of natural non-methane hydrocarbon oxidation on the free radical and ozone budgets above a eucalyptus forest, chemosphere: global change science. Elsevier Science, 3, 353–366, 2001.

Rodgers, C.D. Retrieval of atmospheric temperature and composition from remote measurements of thermal radiation. Rev. Geophys. Space Phys. 4, 609–624, 1976.

Rodgers, C.D. Characterization and error analysis of profiles retrieved from remote sounding measurements. J. Geophys. Res., 5587–5595, 1990.

Rozanov, A. Modeling of the radiative transfer through a spherical planetary atmosphere: application to the atmospheric trace gases retrieval from occultation- and limb-measurements in UV–Vis–NIR. Ph.D. Thesis, Univer-sität Bremen, ISBN 3-8325-0138-X, Logos Verlag Berlin, 2001.

Russel, J.M., Gordley, L.L., Park, J.H., Drayson, S.R., Hesketh, W.D., Cicerone, R.J., Tuck, A.F., Frederick, J.E., Harries, J.E., Crutzen, P.J. The halogen occultation experiment. J. Geophys. Res. 98 (D6), 10777–10797, 1993.

Solomon, S. et al. Visible and near ultraviolet spectroscopy at mcmurdo station, antarctica. 10. Reduction of stratospheric NO_2 due to pinatubo aerosols. J. Geophys. Res.-Atmos. 99, 3509–3516, 1994.

Wayne, R., Barnes, I., Biggs, P., Burrows, J., Canosa-Mas, C., Hjorth, J., Bras, G.L., Moortgat, G., Perner, D., Poulet, G., Restelli, G., Sidebottom, H. The nitrate radical: physics, chemistry, and the atmosphere. Atmos. Environ. A 25, 1–203, 1991.